

SUPERCONDUCTING PHASE-LOCKED LOCAL OSCILLATOR FOR SUBMM INTEGRATED RECEIVER*

V.P. Koshelets^{1,2}, P.N. Dmitriev¹, A.B. Ermakov¹, A.S. Sobolev¹, M.Yu. Torgashin¹,
V.V. Khodos², V.L. Vaks², P.R. Wesselius³, C. Mahaini⁴ J. Mygind⁴,

¹Institute of Radio Engineering and Electronics, Moscow, Russia

²Institute for Physics of Microstructure, Nizhny Novgorod, Russia

³National Institute for Space Research (SRON), Groningen, the Netherlands

⁴Department of Physics, Technical University of Denmark, Lyngby, Denmark

ABSTRACT

Presently a Josephson Flux Flow Oscillator (FFO) appears to be the most developed superconducting local oscillator for integration with an SIS mixer in a single-chip submm-wave receiver [1, 2]. A receiver DSB noise temperature below 100 K has been achieved for a superconducting integrated receiver (SIR) operating with an internal FFO in the frequency range 480 - 520 GHz. The feasibility of phase locking a FFO to an external reference oscillator at all frequencies of interest has to be experimentally proved because it is vitally important for practical use of the SIR in high-resolution spectral studies. The increase of the intrinsic FFO linewidth due to the larger internal damping caused by Josephson self-coupling (JSC) effect at voltages $V > V_{JSC} = V_{gap}/3$ considerably complicates phase locking of the FFO. Comprehensive measurements of the FFO radiation linewidth have been performed using an integrated harmonic SIS mixer; the obtained FFO linewidth and spectral line profile have been compared to theory. The influence of the FFO parameters on the radiation linewidth, particularly the effect of the differential resistances associated both with the bias current and the applied magnetic field has been studied in order to optimize the FFO design. New FFO designs have resulted in a free-running FFO linewidth of about 10 MHz in the flux flow regime up to 712 GHz, limited only by the gap value of the Nb-AlOx-Nb junction. This narrow free-running linewidth along with the construction of a wide-band PLL system has enabled us to phase lock the FFO throughout the frequency range 490 – 712 GHz where continuous frequency tuning is possible. An absolute FFO phase noise as low as -73 dBc and -69 dBc at 100 kHz offset from the carrier has been achieved at 450 and 707 GHz, respectively. This satisfies the requirements for single dish radio astronomy missions and atmospheric monitoring.

*The work was supported in parts by the Russian SSP "Superconductivity", RFBR projects 00-02-16270, INTAS project 01-0367, the Danish Research Academy, the Danish Natural Science Foundation, the Hartmann Foundation, and the Nederlandse Organisatie voor Wetenschappelijk Onderzoek (NWO). Authors thank A. Baryshev, T. de Graauw, M. Khapaev, M. Kupriyanov, A. Pankratov, M. Samuelsen, S. Shitov, H. van de Stadt, A. Ustinov and N. Whyborn for fruitful discussions

Lightweight and compact ultra-sensitive submm Superconducting Integrated Receivers (SIR) [1, 2] with low power consumption are very suitable for both radio-astronomical research and remote monitoring of the Earth atmosphere. The SIR is a single-chip device, which comprises an SIS-mixer with a quasioptical antenna and a superconducting local oscillator. Presently, the Flux Flow Oscillator (FFO) [3] based on unidirectional flow of magnetic vortices in a long Josephson tunnel junction is the best choice for integration with an SIS mixer. Nb-AlO_x-Nb FFO's have been successfully tested as local oscillators from 120 to 700 GHz (gap frequency of Nb) providing enough power to pump an SIS-mixer (about 1 μ W at 450 GHz). Both frequency and power of the FFO can be dc tuned [2, 4]. A receiver DSB noise temperature below 100 K has been achieved for a SIR with the FFO operated in the frequency range 480 - 520 GHz [2, 5]. The antenna beam, approximately f/9 with sidelobes suppressed below -16 dB [2], makes the integrated receiver suitable for coupling to a telescope. An imaging array of nine SIRs has been developed and tested [2, 5].

The frequency resolution of a receiver is one of the major parameters in spectral radio astronomy. In order to obtain the required frequency resolution of at least one part per million and to allow interferometric measurements the local oscillator must be phase-locked to an external reference. In order to study the conditions for phase locking of the FFO linewidth has been measured using a specially developed technique based on an integrated harmonic mixer [6]; see also [2, 4]. An unexplained superfine resonance structure on the FFO IVC was resolved by this technique [7]. This structure considerably complicates FFO phase locking. In order to avoid this structure and to realize permanent frequency tuning (at least along the Fiske steps) we have developed a new design of the FFO. The new FFO is tapered at both ends so that its width is decreased from 6 μ m to 1.5 μ m over a distance of 20 μ m (see Fig. 1). As a result of this modification the resonant structure was almost suppressed. It should be noted that a tapered FFO has larger output impedance compared to the usual FFO of rectangular shape. This also simplifies the impedance matching to the microwave circuits.

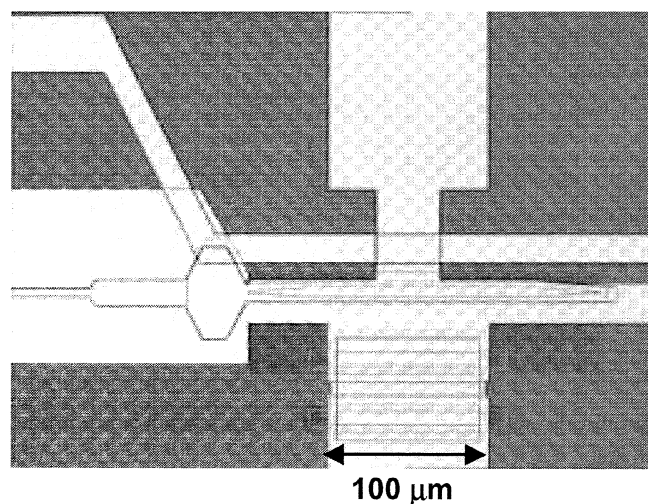


Fig. 1. Photo of the tapered FFO with separate control line for magnetic tuning.

The absence of the resonance structure enables detailed analysis of the free-running FFO spectrum. The FFO line profile has been measured in different regimes of FFO operation and compared to theoretical models. For this we use a frequency locking system with a relatively low loop gain (so called, frequency detector). Thus very low-frequency noise and drift is eliminated by the narrow-band feedback and the “natural” linewidth, determined by much faster fluctuations, can be measured. The shape of the FFO spectrum provides important information about the relationship between internal and external fluctuations as well as the spectral distribution of these fluctuations. According to theory [8, 9] the line shape is Lorentzian for wideband fluctuations, whereas the profile will be Gaussian for narrow-band external electromagnetic interference, e.g. EMI with frequencies smaller than the free-running FFO linewidth δf_{AUT} . A Lorentzian shape of the FFO line has been observed both at higher voltages on the flux flow step (FFS) [10] and at Fiske steps (FS's) [11] in the resonant regime. This means that the free-running FFO linewidth in all operational regimes is determined by wideband thermal and shot noise fluctuations. That is very different from traditional microwave oscillators where the “natural” linewidth is very small and the observed linewidth can be attributed mainly to external fluctuations.

According to theory [8, 9] the radiation linewidth of a small (lumped) Josephson oscillator is determined by the noise spectral power density, $S_I(0)$, of the bias current at low frequencies, $0 < f < \delta f_{AUT}$, where δf_{AUT} is the linewidth of the free-running junction. This noise spectral density is a nonlinear superposition of wide-band thermal and shot noise converted by the Josephson junction to low frequencies [8, 13]. The current noise is transformed into voltage (and consequently, frequency) fluctuations by the differential resistance, $R_d^B = \partial V / \partial I_B$, associated with the bias current I_B . The dependence of the calculate linewidth for the lumped tunnel junction is shown as curve 1 in Fig. 2. The experimental values of the FFO linewidth (asterisks in Fig. 2) are considerably larger than predicted [8, 13, 14]. Furthermore, there is a plateau where the linewidth does not decrease below a few hundreds of kilohertz while R_d^B decreasing below 0.003Ω . To explain such behavior an additional noise contribution is needed; furthermore since the FFO line shape remains Lorentzian at FSs with small R_d^B we can conclude that this extra noise is wideband. Thus the standard noise model for lumped (short) tunnel junction is insufficient to explain the noise associated with the flux flow in the distributed long Josephson junction.

Recently an additional noise term, which accounts for the influence of the wideband noise in the bias current introduced via the magnetic field control line, has been added to form a phenomenological FFO model [11] (see also [15]):

$$\delta f = (2\pi/\Phi_0^2) (R_d^B + K*R_d^H)^2 S_i(0), \quad (1)$$

where $R_d^H = \partial V_{FFO} / \partial I_H$ is the differential resistance associated with the magnetic field, and K is a coefficient of the order of unity. Note that $R_d^H = (\partial V_{FFO} / \partial I_{CL}) / M$, where M is the mutual inductance between the control line and the FFO, I_{CL} is the current in the control line. This model allows us to calculate quantitatively the FFO linewidth in the whole operational range (see Fig. 2 – solid line). The calculated dependence of the linewidth of the lumped tunnel junction [8, 13] for the case of wide-band fluctuations only via I_B ($K = 0$) is shown in Fig. 2 by the dashed line 1), the dependence for fixed values of $R_d^{CL} = 0.003 \Omega$

and $R_d^{CL} = 0.03 \Omega$ are presented by the dotted and the dash-dotted lines 2) and 3), respectively. The solid line is calculated for each experimental point taking into account all relevant parameters (I_B , V , R_d^B , R_d^{CL} , etc.). Indeed the calculations agree with the measured linewidth over the whole range of experimental parameters by using $K=1$ both on the Fiske steps and on the flux flow step. The fact that $K=1$ gives the best fit is not understood, but it may relate to the geometry of the junction and the control line. The increase of the intrinsic linewidth at the R_d^B value of about 0.01Ω is related to the strong increase of the internal damping [12] caused by Josephson self-coupling (JSC) at voltages $V > V_{JSC} = 1/3 * V_{gap}$ (V_{JSC} corresponds to 450 GHz for Nb-AlO_x-Nb FFO). As a result the FFO IVCs are deformed at V_{JSC} (see Fig. 4 below) and R_d^{CL} increases. The dependence of the FFO radiation linewidth on R_d^{CL} is shown in Fig. 3

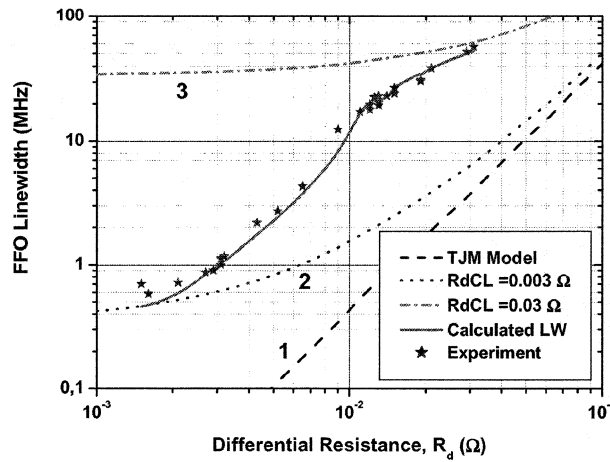


Fig. 2. Dependence of FFO radiation linewidth on the bias current differential resistance R_d^B . Curves 1 - 3 are calculated for the following parameters: $V_{dc} = 1$ mV, $I_{qp} = 3$ mA, $I_s = 7$ mA, $T_{eff} = 4.2$ K.

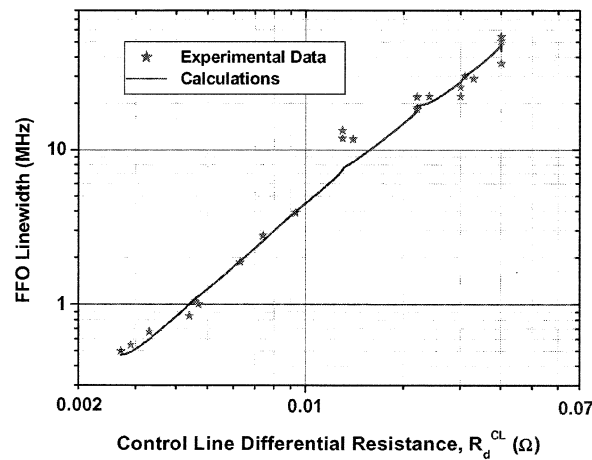


Fig. 3. Dependence of the FFO radiation linewidth on the control line differential resistance R_d^{CL} . The solid curve is calculated for each experimental point for measured parameters (I_B , V , R_d^B), $T_{eff} = 4.2$ K.

In order to phase lock the FFO one has to decrease the free running linewidth, which (in accordance to Eq. 1 and Fig. 2, 3) is mainly determined by R_d^B and R_d^{CL} . New designs of the FFO have been developed to achieve this, one design is shown in Fig. 1. A typical set of the corresponding FFO IVCs is shown in Fig. 4. Data were recorded with incremented magnetic field. Each IVC was measured for a fixed control line current, I_{CL} , which is then incremented by $\Delta I_{CL} \approx 0.5$ mA before the next IVC is recorded. The dependence of the R_d^B and R_d^{CL} on the FFO voltage is shown in Fig. 5.

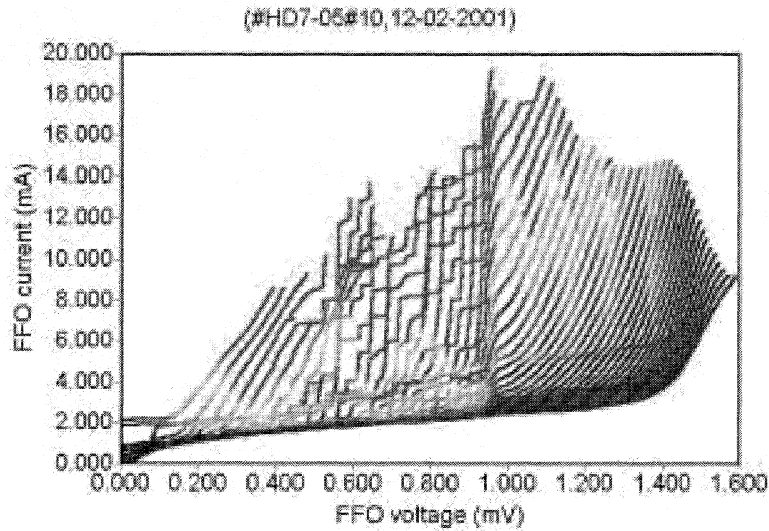


Fig. 4. IVCs of the FFO with new design, measured with incremented magnetic field ($I_{CL} = 10\text{--}35$ mA)

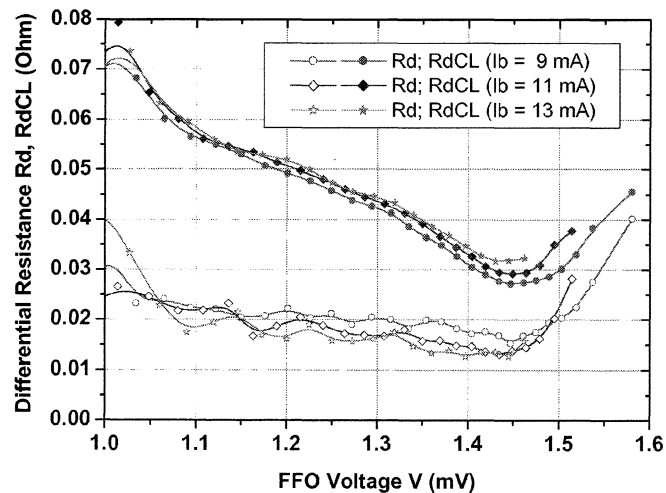


Fig. 5. Dependence of the differential resistances R_d^B and R_d^{CL} on FFO voltage, measured at different bias currents, I_B .

Fig. 5 shows a well-defined dependence of R_d^{CL} on bias voltage (FFO frequency). This has been observed for all tested FFO of very different designs and may be considered as universal and fundamental. Presumably it reflects the fact that introduction of an additional fluxon in the junction requires increasing control line current as the fluxon chain gets denser. One can see that R_d^{CL} has a minimum at 1.45 mV (corresponding to a FFO frequency of 725 GHz). The position of this minimum approximately coincides with $V_g/2$ and changes with temperature as V_g . At $I_B = 11$ mA the R_d^{CL} value increases considerably from 0.03Ω (that results in free-running linewidth of about 5 MHz) to almost 0.08Ω at 500 GHz (1.03 mV). The free-running FFO linewidth correspondingly increases almost 10 times that considerably complicates the phase locking of FFO. Note that the JSC effect is important only for $0.9 \text{ mV} < V < 1.1 \text{ mV}$.

The FFO, as any Josephson junction, is a perfect voltage-controlled oscillator and hence its frequency can be stabilized and the FFO linewidth can be decreased by phase locking to an external reference source using a phase-lock loop (PLL) system with bandwidth larger than δf_{AUT} . Actually, a PLL system will effectively suppress the influence from external low frequency fluctuations and alter the differential resistances R_d^B and R_d^{CL} in the bias point. We have developed a special PLL unit utilizing an integrated SIS harmonic mixer to down-convert the FFO signal to a 400 MHz IF signal. After amplification the IF signal is compared to a 400 MHz reference signal in an analog phase detector, the output of which is fed to the FFO bias supply. All reference signals as well as the spectrum analyzer used to display the phase noise on the IF signal are phase-locked to a common 10 MHz reference oscillator. The PLL unit is optimized for operation with a low signal-to-noise ratio at a minimal time delay (measured delay of about 5 ns corresponds to a regulation bandwidth of 50 MHz). The bandwidth of the complete PLL system, Δf_{PLL} , is further limited to 15 MHz due to the delay in its 2 m long cables, but it still exceeds the free-running linewidth of the FFO with new design.

Earlier, phase locking of a Josephson oscillator was demonstrated in the frequency range 250 – 450 GHz [16] for a FFO biased on resonant Fiske steps. In this case the initial free-running FFO linewidth (FWHP, full width, half power) was only about 1 MHz due to the low dynamic resistance of the Fiske resonances. The new design of the FFO [10, 11] results in a decrease of the free-running FFO linewidth in the flux flow regime for $V > V_{JSC}$. Along with development of an improved wideband PLL system it enables us to phase lock FFO in the frequency range from 490 to 712 GHz, limited only by the gap value of the Nb-AlOx-Nb junction. Fig. 7 demonstrates the spectra of the frequency and phase locked FFO operating at 707 GHz. The wings at the curve "A" of Fig. 7a mark the frequency difference from the carrier at which the phase of the return signal from PLL system is shifted by $\pi/2$ that results in some increase of the phase noise.

The PLL system, of course, cannot change the wide-band thermal and shot noise fluctuations, but it can diminish both differential resistances (at frequencies $f < \Delta f_{PLL}$) to zero. This manifests itself as a constant-voltage step in the dc I-V curve of the FFO. Note that a similar step with finite slope and larger voltage and current span appears when the FFO is only frequency locked (see Fig. 6). The voltage locking range here is about 5 μV corresponding to a frequency range of about 2.5 GHz.

According to Eq. (1) the zero dynamic resistance created by the PLL system results in an infinitely sharp spectral line. Indeed, as seen in Fig. 7 b, a 1 Hz linewidth is measured at 707 GHz relative to the reference oscillator. The 1 Hz is an artifact caused by the limited frequency resolution of the spectrum analyzer. One can see that the residual phase noise is as low as 75 dB below the carrier. The dependence of the phase noise on the frequency offset from the carrier is shown with diamonds in Fig. 8. Even lower phase noise has been measured for a FFO in the resonant regime when biased on the steep Fiske steps, $f = 450$ GHz (see Fig. 8). In order to find the “absolute” (total) phase noise of the phase-locked FFO one should add the noise of the reference oscillator multiplied by n^2 where n is the harmonic number used in the harmonic mixing. The absolute FFO phase noise (solid lines in Fig. 8) is dominated by the reference oscillator noise for offsets < 1 MHz. Note that the measured phase noise already meets the requirements for single dish radio astronomy and atmospheric missions. It should be mentioned that the phase noise at large offsets probably is limited by the measuring system rather than by the FFO itself.

Since the free-running FFO line shape is Lorentzian, the FFO power inside the effective PLL regulation bandwidth can be calculated, see Fig. 9. From this figure one can see that the initial FFO linewidth should not exceed 3.5 MHz to insure that the phase-locked FFO oscillates with 90% of the total power. The present set-up has an effective PLL bandwidth of about 15 MHz. The “unlocked” rest of the total FFO power will increase both the phase noise (compare curves with different free-running linewidth in Fig. 8) and the calibration error. The calibration error of the spectrometer noise temperature will be approximately equal to the percentage of the unlocked FFO power. To overcome this problem an additional decrease of the FFO free-running linewidth (new designs with smaller R_d^B and R_d^{CL}) and an increase of the PLL regulation bandwidth are required. In this respect the ongoing design of a new ultra-wideband PLL system that can operate at cryogenic temperature seems very promising.

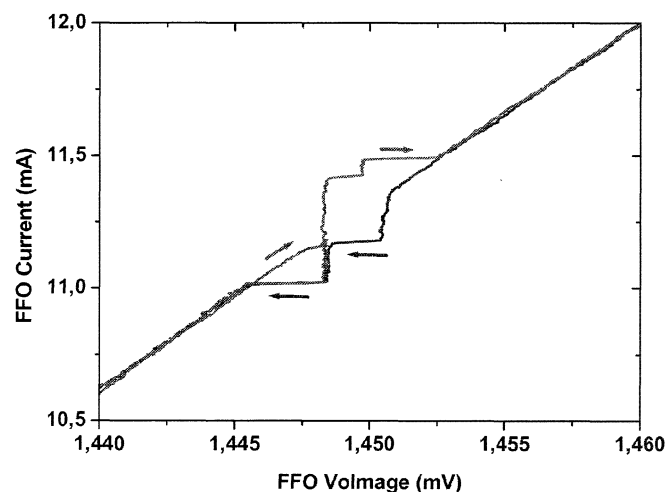


Fig. 6. IVC of a FFO, frequency locked at 700 GHz.

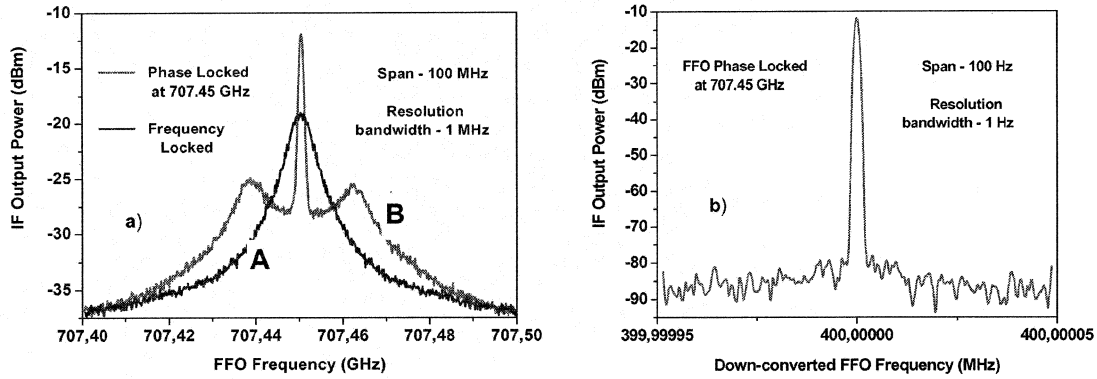


Fig. 7. Residual spectra of a FFO operating at 707.45 GHz. (a) Frequency locked FFO (A) and phase-locked FFO (B); the free-running linewidth is $\delta f_{AUT} = 6.3$ MHz, spectrum analyzer span 100 MHz. (b) Down-converted spectrum, span 100 Hz. $T = 4.2$ K

In order to resolve a weak signal adjacent to a strong line the PL FFO must have a well-defined line-shape. The dynamic range of the spectrometer is closely related to the ratio between the carrier and the spectral power density (FFO phase noise) at a frequency offset equivalent to the channel spacing of the spectrometer. The phase noise of the phase-locked FFO is about -80 dBc/Hz at the 1 MHz offset from the carrier for $f_{FFO} = 700$ GHz (see Fig. 8). For a 1 MHz channel this gives a dynamic range of 20 dB for the spectrometer. This figure exactly corresponds to the requirements for the HIFI wide band spectrometer (WBS).

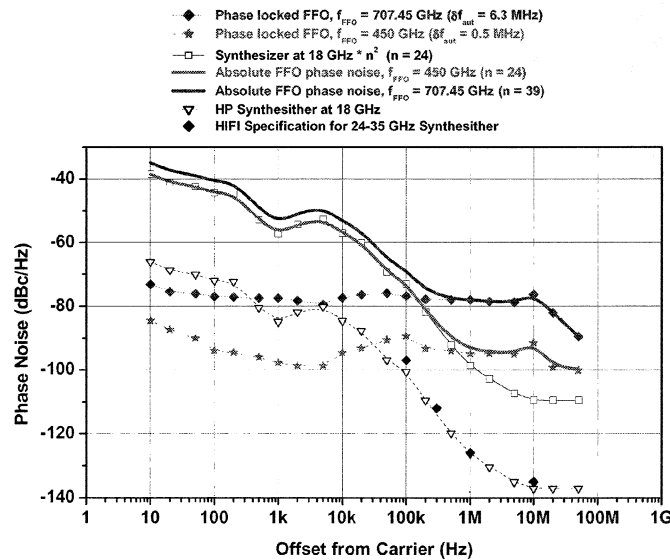


Fig. 8. Phase noise of a phase-locked FFO measured at different frequencies. Since the phase noise of the FFO is measured relative to the n^{th} harmonic of a synthesized oscillator, its noise, multiplied by a factor n^2 , should be added to the residual FFO noise to get the total (absolute) FFO phase noise – solid and dash lines.

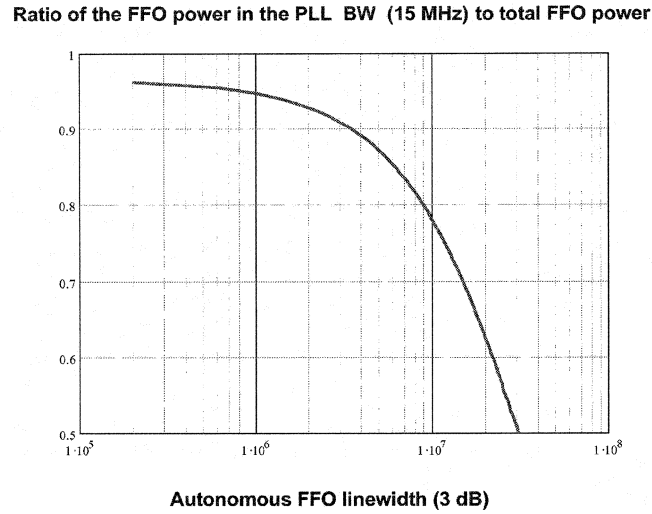


Fig. 9. Dependence of the ratio of phase-locked FFO power to total power emitted on the autonomous 3 dB linewidth, calculated for a Lorentzian line shape and an effective PLL BW = 15 MHz.

The noise level of a phase-locked FFO at an offset from the carrier equal to the receiver intermediate frequency (IF) will couple to the SIS mixer and raise the SIR noise level. Usually the IF (say, 4–8 GHz) is far above the PLL regulation bandwidth (< 100 MHz), the phase noise of the synthesizer and PLL will not contribute to the FFO noise. However, for safe calculations of the requirements for FFO noise at large offsets we may assume that this noise, T_{LO} , contributes less than 10% of the receiver noise (say $T_R = 200$ K at 650 GHz, so $T_{LO} < 20$ K). This value of T_R corresponds to a value of about $0.65 \cdot hf/k_B$ at $f = 650$ GHz, where h and k_B are Planck's and Boltzmann's constants, respectively. The carrier power can be estimated as the power required for pumping a SIS mixer at a specified frequency. The optimal FFO power delivered to the mixer at the LO frequency is

$$P_{LO}^{opt} = (\alpha \cdot hf_{LO})^2 / (e^2 \cdot R_{rf}), \quad (2)$$

where R_{rf} is the SIS mixer high frequency resistance (approx. the normal state resistance, say 10Ω) and $\alpha = 0.8$. For $f_{LO} = 650$ GHz $P_{LO}^{opt} = 460$ nW. The allowed noise/carrier ration (NCR) can be calculated as

$$NCR = 10 \log (T_{LO} \cdot k_B) - 10 \log (P_{LO}^{opt}) = -152 \text{ dBc/Hz}. \quad (3)$$

Certainly such low phase noise cannot be directly measured by any available technique. Indirectly, however, we already did this when we compared the noise temperature of the integrated receiver pumped by an internal FFO and an external local oscillator and carefully estimated the receiver noise temperature budget. Within the accuracy of the measurements we can conclude that the FFO did not add to the receiver noise temperature more than 20 K at an IF = 1-2 GHz. It should be noted that balanced mixers reject the LO noise to some degree and will further diminish the LO noise.

In conclusion, a considerable narrowing of the free-running FFO linewidth (compared to all previous measurements) along with the construction of a wide-band PLL system have enabled us to phase lock a Nb-AlO_x-Nb FFO in the frequency range 490 – 712 GHz where continuous frequency tuning is possible. An absolute FFO phase noise as low as –73 dBc and –69 dBc at 100 kHz offset from the carrier has been achieved at 450 and 707 GHz, respectively. This satisfies requirements for single dish radio astronomy missions and atmospheric monitoring.

References

- [1] V.P. Koshelets, S.V. Shitov, L.V. Filippenko, A.M. Baryshev, H. Golstein, T. de Graauw, W. Luinge, H. Schaeffer, and H. van de Stadt, *Appl Phys Lett*, **68**, 1273 (1996).
- [2] V.P. Koshelets and S.V. Shitov, *Superconductor Science and Technology*, **13**, R53 (2000).
- [3] T. Nagatsuma, K. Enpuku, F. Irie, and K. Yoshida, *J Appl Phys*, **54**, 3302 (1983), see also Pt. II: *J Appl Phys* **56**, 3284 (1984); Pt III *J Appl Phys* **58**, 441 (1985); Pt IV *J Appl Phys* **63**, 1130 (1988).
- [4] V.P. Koshelets and J. Mygind, “Flux Flow Oscillators For Superconducting Integrated Submm Wave Receivers”, *Studies of High Temperature Superconductors*, edited by A.V. Narlikar, NOVA Science Publishers, New York, vol. 39, pp. 213-244, (2001).
- [5] S.V. Shitov, A.B. Ermakov, L.V. Filippenko, V.P. Koshelets, A.M. Baryshev, W. Luinge, and J.-R. Gao, *IEEE Trans on Appl Supercond.*, **9**, 3773 (1999).
- [6] V.P. Koshelets, S.V. Shitov, L.V. Filippenko, A.V. Shchukin, and J. Mygind, *Appl Phys Lett*, **69**, 699 (1996).
- [7] V.P. Koshelets, A.B. Ermakov, S.V. Shitov, P.N. Dmitriev, L.V. Filippenko, A.M. Baryshev, W. Luinge, J. Mygind, V.L. Vaks, D.G. Pavel’ev, *Proceedings of the 11th International Symposium on Space Terahertz Technology*, University of Michigan, Ann Arbor. May 1-3, (2000), pp 532-541.
- [8] K.K. Likharev, “Dynamics of Josephson junctions and circuits” *Gordon and Breach Science Publishers* (1986).
- [9] A.N. Malakhov, “Fluctuations in auto-oscillating systems”, Science, Moscow, 1968 (in Russian).
- [10] V.P. Koshelets, S.V. Shitov, P.N. Dmitriev, A.B. Ermakov, L.V. Filippenko, V.V. Khodos, V.L. Vaks, A.M. Baryshev, P.R. Wesselius, J. Mygind, *Physica C*, **367**, pp. 249 - 255, (2002).
- [11] V.P. Koshelets, A.B. Ermakov, P.N. Dmitriev, A.S. Sobolev, A.M. Baryshev, P.R. Wesselius, and J. Mygind, *Extended Superconductor Science and Technology*, v. **14**, pp. 1040 - 1043, (2001)
- [12] V.P. Koshelets, S.V. Shitov, A.V. Shchukin, L.V. Filippenko, J. Mygind, and A.V. Ustinov, *Phys Rev B*, **56**, 5572 (1997).
- [13] A.J. Dahm, A. Denenstien, D.N. Langenberg, W.H. Parker, D. Rogovin, and D.J. Scalapino, *Phys Rev Lett*, **22**, 1416 (1969).
- [14] M. Salerno, M.R. Samuelsen, and Y. Yulin, *Phys. Rev. B*, v. **86**, pp. 5397-5399, (2001)
- [15] A.L. Pankratov, *Phys. Rev. B*, v. **65**, 054504-1-9, (2002).
- [16] V.P. Koshelets, S.V. Shitov, L.V. Filippenko, V.L. Vaks, J. Mygind, A.B. Baryshev, W. Luinge, and N. Whyborn, *Rev of Sci Instr.*, **71**, 289 (2000).